

High Q Nanoplasmonic biosensor based on surface lattice resonances in the visible spectrum

Arslan Asim^{1*}, Michael Cada^{1,2}, Yuan Ma¹, Alan Fine³

¹Department of Electrical and Computer Engineering, Dalhousie University, Halifax, Canada; arslanasim@dal.ca (A.A.).

²Faculty of Materials Science and Technology, VSB-Technical University of Ostrava, 708 00 Poruba, Ostrava, Czech Republic.

³Department of Physiology and Biophysics, Dalhousie University, Halifax, Canada.

Abstract: Plasmonic nano-antennas are widely accepted as suitable platforms for biosensing tasks because Surface Plasmon Resonance (SPR) is very sensitive to changes in its environment. However, recent studies suggest that SPRs may have limited Quality (Q) factors, especially in comparison with their dielectric counterparts. Therefore, this paper attempts to innovate the design of plasmonic nano-antennas to achieve high Q factors through Surface Lattice Resonance (SLR) in the visible frequency band. This resonance is linked with plasmonic nanostructures organized in arrays. The structure consists of a metal-dielectric-metal configuration at the base with metallic nanopillars protruding upward. The nanophotonic device has been investigated for refractometric sensing applications. The maximum Q factor achieved as a result of this work is 245, which has been compared with contemporary plasmonic metasurface Q factors. The simulation framework has been implemented in COMSOL Multiphysics, which employs the Finite Element Method (FEM). Regression analysis has been used to formulate the calibration curve for the sensor. High Q factors provide better selectivity for biosensing applications.

Keywords: Finite element analysis (FEA), Metamaterial, Plasmonics, Quality (Q) factor, Refractive index, Sensor.

1. Introduction

Nanoscience remains one of the greatest wonders of the twenty-first century. It utilizes knowledge from multidisciplinary research fields to enhance its viability and practicality. A conspicuous domain of nanoscience is nanophotonics which involves the interaction of light with matter designed at nanometer scale. This interaction has been studied and documented for a wide variety of applications including computing, communications, healthcare and environmental control [1, 2]. In this paper, we focus on the application of nanophotonics in sensor technology.

Sensors play a significant role in the monitoring and evaluation of engineering systems. Traditionally, a sensor has been defined as a device that converts a physical, chemical or biological parameter into an electrical signal [3]. However, photonic sensors have an enormous role to play in today's time. Photonic systems are generally faster than electronic systems because of the speed of electromagnetic waves. Nanophotonic sensors are also less bulky compared to traditional optical sensors. They provide smaller footprints as well [4, 5]. A special class of micro/nanophotonic sensors comprises plasmonic materials. The concept of a plasmonic material was presented by Veselago [6]. His theoretical contribution described a material with negative values of permittivity and permeability. In this era, there is a remarkable emphasis on the engineering of novel optical materials. Plasmonic and other types of novel optical materials are collectively known as metamaterials today [6, 7].

Metamaterials have been frequently used for the development of miniaturized optical sensors. Naib et al. have extensively reported sensors employing resonating metamaterial structures. A large portion

of their work is based on plasmonic biosensors in the terahertz frequency band [8, 9]. Similarly, Patel, et al. [10] have studied various metamaterial designs, with special focus on graphene and plasmonics [10, 11]. Several applications have been targeted by photonic metamaterial sensors. Different parameters of blood have been investigated through metaphotonic biosensors [12, 13]. The detection of microorganisms associated with fatal diseases have also been reported in the realm of biophotonic metasensors [14, 15]. Biomedical sensors employing metamaterial structures have been proposed for cancer detection too [16, 17]. Various other biomedical applications have been explored in the context of metamaterial optics. Plasmonic sensors have also shown good promise in the sensing of analytes for various other arenas like environmental monitoring and food industry [18, 19].

This area is witnessing great interest from researchers as many new metamaterial ideas are being proposed for sensing applications. Another well-acknowledged category of metamaterial sensors consists of dielectric sensors. As opposed to plasmonics, dielectric structures suffer from lower losses and provide ease of fabrication due to their compatibility with Complementary Metal-Oxide Semiconductor (CMOS) processes. In terms of sensing performance, plasmonic sensors usually display higher values of sensitivity compared to dielectric sensors. This is because SPR is very sensitive to changes in its environment. However, higher quality factors can easily be achieved by virtue of dielectric resonators, which appears to be a challenge for plasmonic sensors [20–22]. Hence, this paper concentrates on the enhancement of quality factors in plasmonic sensors.

The fundamental concept behind a plasmonic resonance is a metal-dielectric interface. A metal-dielectric interface gives rise to a special phenomenon known as Surface Plasmon Resonance. Two commonly reported types of plasmonic resonances are Surface Plasmon Polariton (SPP) and Localized Surface Plasmon Resonance (LSPR). In the former case, strong electromagnetic fields are observed along the boundary of a metal and dielectric. On the other hand, when strong fields are confined within nanoscale structures, we call it LSPR. The interaction between nanostructures and light is on a subwavelength scale, which requires the size of nanostructures to be smaller than the wavelengths of incident electromagnetic beams. Plasmonic nanostructures can be arranged periodically on larger surfaces to engineer light wavefronts. These flat optical surfaces are called metasurfaces. The term ‘metasurface’ represents a two-dimensional counterpart of the term ‘metamaterial’, which is used to refer to any artificially engineered material with unnatural characteristics. Arrays of periodic nanophotonic resonators give rise to combined resonances termed as Surface Lattice Resonances (SLRs). Generally, in the case of LSPR, the frequency response has a low Quality (Q) factor. On the other hand, collaborative plasmonic resonances originating from nanoplasmonic arrays have larger Q factors. Therefore, Q factor has been a question of interest in the context of plasmonic metasurfaces, especially because of their widespread applications in bioimaging, biosensing, cloaking, etc [23–25].

In this paper, a novel SLR sensor design has been targeted. The proposed sensor operates in the visible light band and provides sharp reflection dip in the targeted frequency range. We emphasize that quality factors have not come into detailed discussion in the context of plasmonic biosensors. Therefore, this paper includes a deep insight into the Q factor of plasmonic metasurface sensors. This is one aspect of this paper’s novelty. The Q factor achieved through the proposed design competes among the highest quality factors reported till date. A comparison table (Table 1) validates the claim. The sensor performance, involving measurement of frequency shifts with changing refractive indices, has been discussed in detail. The simulation work has been carried out in COMSOL Multiphysics. It uses Finite Element Method (FEM) for solving electromagnetic problems. Data analysis and visualization has been done in Python.

Table 1.
Comparison of the proposed work with different meta-photonic sensors.

Ref.	Wavelength/ frequency	Materials	Structure	Signal Response	Maximum Q Factor
Singh, et al. [26]	633 nm	Ag, Si ₃ N ₄ , BP	Planar waveguide	Resonance angle	131.51
Maurya, et al. [27]	11 – 13 THz	Au, SiO ₂	Square patch with triangular edges.	Absorption peak	-
Asim and Cada [28]	1800 – 2200 nm	Ag, SiO ₂	Nanocylinders	Absorption peak	49.99
Asim, et al. [29]	0 – 1 THz	Al, Au, Cu, SiO ₂	Split Ring Resonator	Absorption peak	-
Chen, et al. [30]	1000 – 4500 nm	Au, SiO ₂	Nano-rings	Reflection minima	-
Ni, et al. [31]	700 – 1300 nm	Au, SiO ₂	Dimer (square brackets)	Reflection minima	548
Wang, et al. [32]	0 – 6 THz	Cu, Rogers RT5880	Corrugated rings	Transmission peaks	161.6
Danaie, et al. [33]	1000 – 2000 nm	Ag, Air	8-shaped resonator	Transmission peaks	247.4
Chau, et al. [34]	300 – 1300 nm	Ag, dielectric	Combination of nanosphere and nanorod	Transmission minima	-
Liu, et al. [35]	140 – 200 THz	MgF ₂ , Au, SiO ₂	Nano-disks	Absorption peak	-
Rakhshani and Mansouri-Birjandi [36]	1000 – 4000 nm	Ag, Air	Nanorods	Transmission peaks	-
Kabashin, et al. [37]	400 – 1400 nm	Au, SiO ₂	Nanorods	Reflection minima	-
Wu, et al. [38]	633 nm	Au, SiO ₂ , graphene	Layered films	Resonance angle	-
Xi, et al. [39]	400 – 800 nm	Ag, SiO ₂	Triangle	Transmission peak	-
Mesch, et al. [40]	1000 – 2200 nm	Au, SiO ₂	Rectangular nanoantennas	Transmission minimum	-
This work	480-490 nm	Au, SiO ₂	Nanocylinders	Absorption peaks	245

2. Design and Analysis

The proposed nanostructure design is shown in Figure 1. The structure consists of a metal-dielectric-metal base. The metal-dielectric boundary serves as the resonant cavity that supports plasmon modes. Metal-dielectric-metal structures can provide higher sensitivity and much better resolution. Gold (Au) nano-cylinders are mounted onto the base. The metal used in the base is gold while SiO₂ is the dielectric. The figure also shows the geometrical dimension labels. Table 2 provides the values for the geometrical dimensions. These dimensions have been finalized after a considerable number of trial simulations. The relative permittivity of SiO₂ is considered equal to 2.1. The plasmonic optical properties, predicted by the Drude model, have been used for Au. In Eq. 1, ϵ and ω denote relative permittivity and angular frequency, respectively. The plasma frequency, ω_p equals 13.8×10^{15} rad/s whilst the damping constant, γ is 0.011×10^{15} rad/s for the specific case under consideration (i.e. gold) [41].

$$\epsilon(\omega) = \left(1 - \frac{\omega_p^2}{\omega^2 + \gamma^2}\right) + j \left(\frac{\gamma\omega_p^2}{\omega(\omega^2 + \gamma^2)}\right) \quad (1)$$

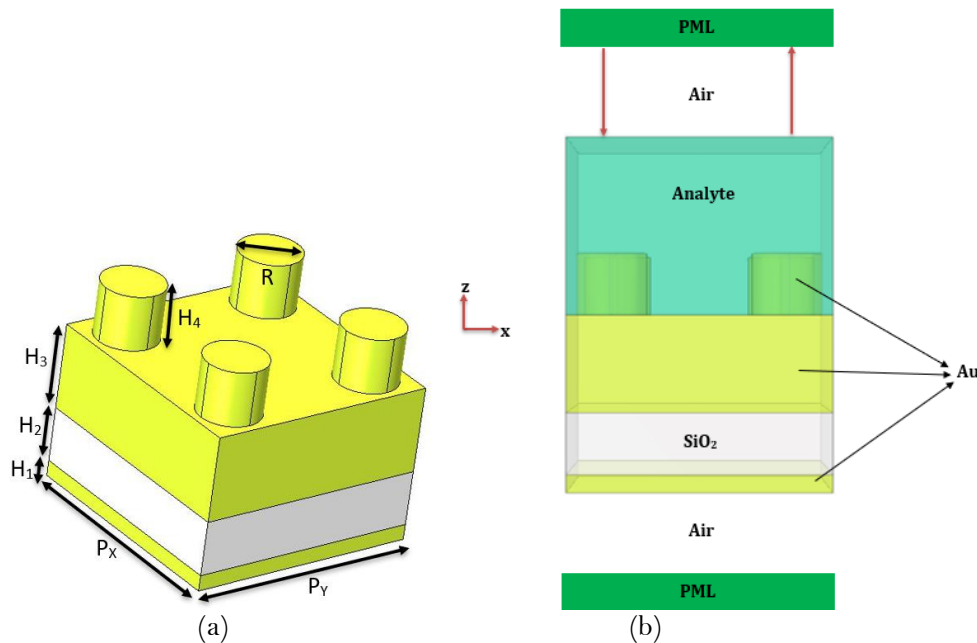


Figure 1. (a) Nanostructure sensing element. (b) Simulation setup.

Table 2.

List of geometrical symbols and their values.

Dimension	Value	Dimension	Value
P (P _X , P _Y)	300 nm	R	40 nm
H ₁	20 nm	H ₂	70 nm
H ₃	110 nm	H ₄	70 nm

Figure 1(b) shows the simulation setup. Perfectly Matched Layers (PMLs) are defined on both sides of the structure. The bottom face of the upper PML is used as ‘port 1’ to supply electromagnetic waves. The upper face of the lower PML is defined as ‘port 2’. Computational simulations have been performed through Finite Element Method (FEM). The Finite Element Analysis (FEA) is implemented in COMSOL Multiphysics. The physics used for the simulations is ‘Electromagnetic Waves, Frequency Domain’. There is air between lower PML and lower end of the sensor. The space around the four nanocylinders has been allocated for the analyte, the chemical that needs to be sensed. The height of the analyte chamber (in the z direction) is 200 nm. It spans across the sensor in the x and y directions. The air gap is 800 nm long on each side of the structure and the PML thickness in 125 nm. Periodic boundary conditions are applied in the x and y directions. The electromagnetic source emits x-polarized visible light waves along the negative z axis. The outer surfaces of both the PMLs have scattering boundary conditions applied to them. A wavelength sweep has been used to study the response of the sensor with changing wavelengths. The wavelengths range from 480 nm to 490 nm.

S parameters are recorded and used to obtain reflectance, transmittance and absorptance of the metasurface in accordance with the expressions mentioned below.

$$A(\omega) = 1 - R(\omega) - T(\omega) \tag{2}$$

$$R(\omega) = |S_{11}|^2 \tag{3}$$

$$T(\omega) = |S_{21}|^2 \tag{4}$$

In Figure 2, the frequency dependent response of the sensor has been depicted. A resonance peak is evident in the absorption spectrum. The peak appears in the visible light regime. It corresponds to a

wavelength of 481.92 nm. This wavelength point belongs to an analyte with refractive index of 1.33. When the analyte refractive index changes, the wavelength peak shifts as shown later in the paper.

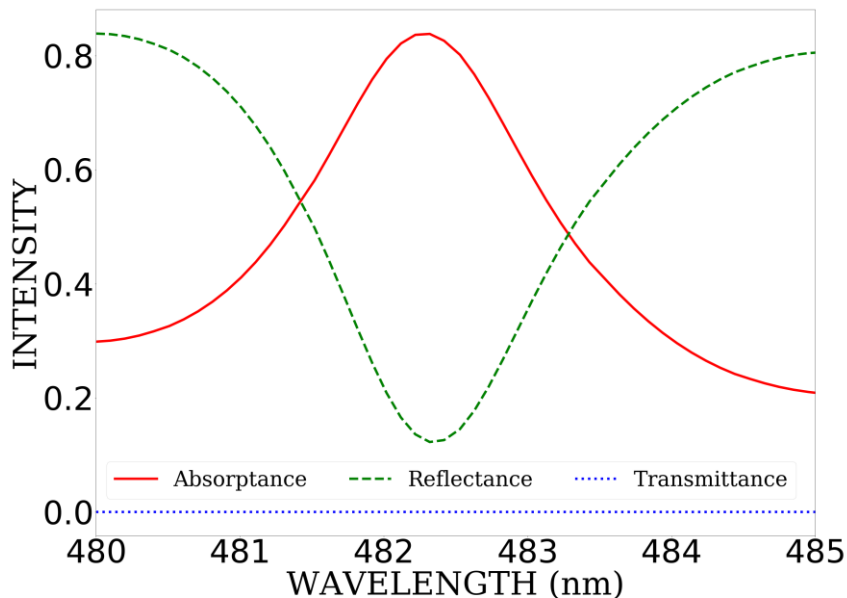


Figure 2.
Spectral response of the nanophotonic sensor.

Figure 3 shows the distribution of electromagnetic fields in the nano-resonator. The electric and magnetic field distributions at the upper surface of the structure, upon which the nanopillars stand, have been shown. The Surface Lattice Resonance (SLR) is evident at the resonance peak. The SLR results in field confinements around the edges of the nanostructures. The SLR is a unique phenomenon combining the optical field localization effect of individual plasmonic nanostructures as well as the diffraction effect resulting from the interaction of electromagnetic waves with the metasurface array. The confinement of electromagnetic fields inside individual nanoparticles is referred to as Localized Surface Plasmon Resonance (LSPR). Though it provides high sensitivity, the associated quality factor is usually of the order 10. SLR provides a wonderful opportunity to combine the sensitive nature of plasmonic resonance with higher Q factors.

In many applications, higher quality factors are desirable. High Q factor indicates smaller losses. When the Q factor is high, there is large amount of energy concentrated in the resonance. In other words, a good Q factor guarantees that the ratio of energy stored to energy lost is high. Hence, a sensor with a higher Q factor will display better spectral selectivity.

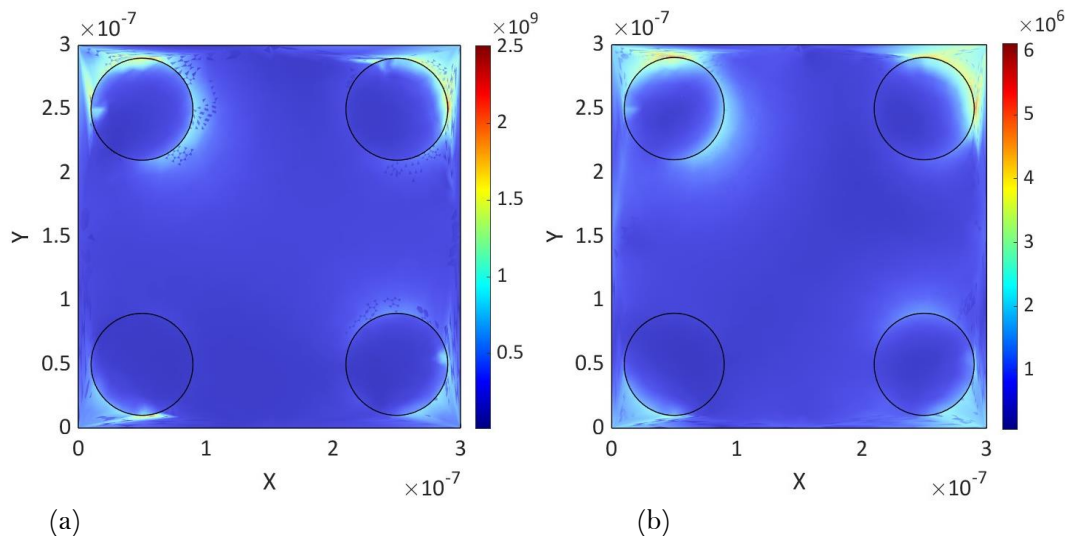


Figure 3. Normalized (a) electric (V/m) and (b) magnetic (A/m) fields' distribution plots at the resonant wavelength.

The proposed design can be employed in biosensing applications by using a visible light transceiver. Visible light wavelengths can be incident on the structure and reflectivity can be measured. A reflection dip can be spotted for each refractive index being sensed. The shifts in the two reflection dips can be tracked to detect refractive index.

3. Application

Next, the performance of the sensor has been gauged and recorded. Very minute refractive index changes have been introduced in the analyte medium to see the effect on resonant wavelength. The step size for refractive index variation is 0.005. The resonance spectrum tends to shift towards the right (higher wavelengths) with increasing refractive index. The resonant wavelengths for 5 different refractive index media have been plotted. Subsequently, linear regression analysis has been applied. Figure 4 (a) and (b) depict the above-mentioned details. Figure 4 (a) shows the spectra for different refractive indices while (b) provides linearized response of the sensor in the given refractive index range. Figure 4 (c) provides a similar linearized response. The variables in Figure 4 (c) are resonant wavelength and concentration of aqueous potassium ion concentrations. The case of potassium ion concentration holds a lot of significance from a clinical perspective. For example, accurate detection of potassium ion concentration in blood/ serum/ urine can be a critical step in determining if a patient has hyper/ hypokalemia.

$$n = 1.3352 + 0.0016167 \frac{Ck}{529.8} - 0.0000004 \left(\frac{Ck}{529.8} \right)^2 \quad (5)$$

Equation (5) describes the relationship between the concentration (C in mg/dL) of potassium ion solution and the refractive index (n). The constant, k, is the concentration element. Its value is 50 for K⁺ solutions. The values of the refractive indices for different concentrations have been calculated through Eq. 5 and fed into the simulation model. The resulting simulation data have been used to plot Figure 4 (c).

Besides the high Q factor, the sensor provides good sensitivity and very linear response. The correlation coefficients (R values) for Figure 4 (a) and Figure 4 (b) are 0.9999502842624352 and 0.9998633442553864, respectively. These values serve as evidence of sensor linearity. The constants m₁ and m₂ are equal to 338 nm/ RIU and 484 nm/ (mg/dL), respectively. RIU stands for Refractive Index Unit. Both constants signify the sensitivity of the nanophotonic structure. The constants c₁ and c₂ are y-intercepts of the regression lines of best fit.

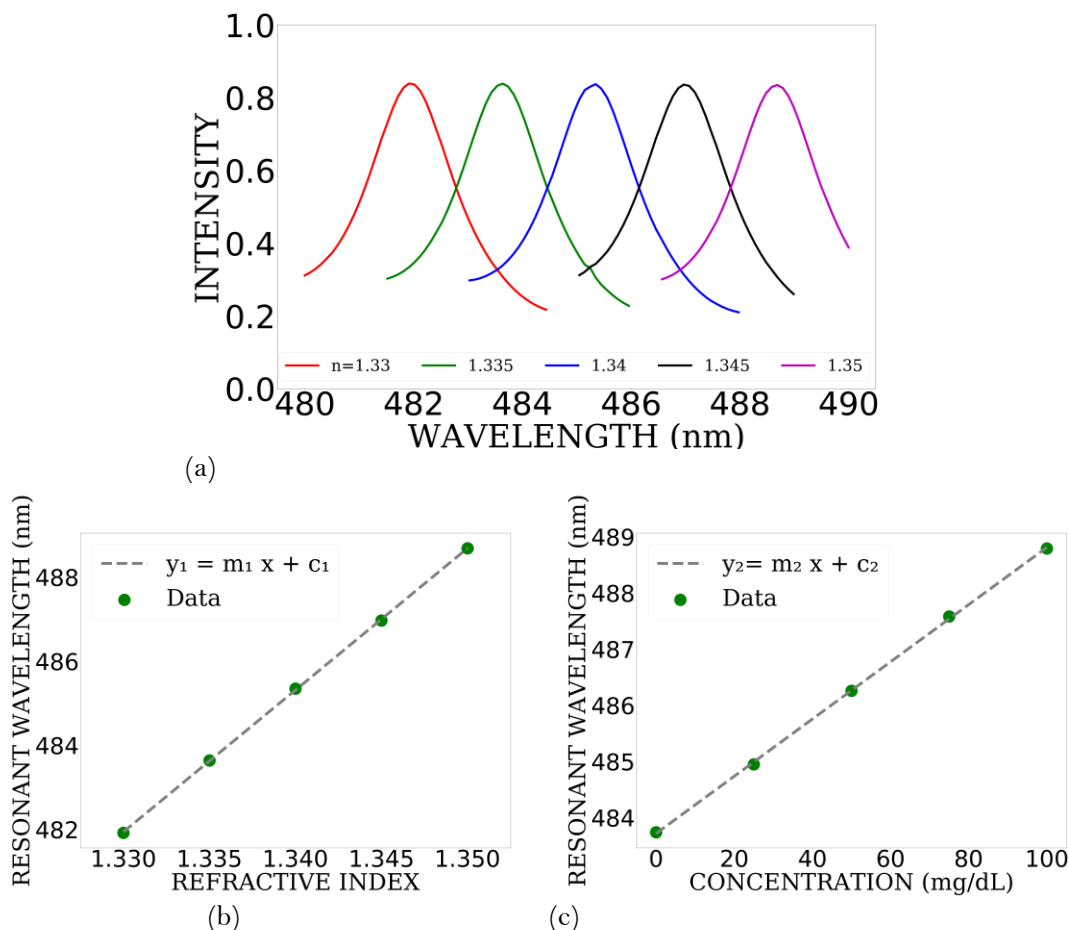


Figure 4.

(a) Resonance spectra for different refractive indices of the analyte. (b) Resonant wavelength plotted against the refractive index of the analyte. Data points have been extracted from the spectra in (a). (c) Resonant wavelength plotted against concentration of potassium ion solutions. magnetic (A/m) fields' distribution plots at the resonant wavelength. Regression analyses have been applied to calibrate the responses in (b) and (c).

5. Conclusion

In this paper, we have provided a quick overview of the recent works on plasmonic sensors, especially in the context of their Q factors. It has been identified that the achievement of high Q factors through plasmonic devices is an area of potential improvement. Therefore, a novel design has been presented that utilizes Surface Lattice Resonance (SLR) in the visible region to achieve a Q factor of 245. This is significantly higher than Localized Surface Plasmon (LSP) sensors. High Q factors can provide better selectivity in biosensing applications.

Transparency:

The authors confirm that the manuscript is an honest, accurate, and transparent account of the study; that no vital features of the study have been omitted; and that any discrepancies from the study as planned have been explained. This study followed all ethical practices during writing.

Acknowledgments:

This work was supported by NSERC (Natural Sciences and Engineering Research Council) of Canada. The work of Arslan Asim was supported by Research Nova Scotia (RNS) and Dalhousie University.

Copyright:

© 2025 by the authors. This open-access article is distributed under the terms and conditions of the Creative Commons Attribution (CC BY) license (<https://creativecommons.org/licenses/by/4.0/>).

References

- [1] 21st Century Nanoscience - Book Series, "Routledge & CRC Press," Routledge.com," Retrieved: <https://www.routledge.com/21st-Century-Nanoscience/book-series/CRCNANO>. [Accessed Feb. 05, 2025], 2020.
- [2] S. Malik, K. Muhammad, and Y. Waheed, "Nanotechnology: A revolution in modern industry," *Molecules*, vol. 28, no. 2, p. 661, 2023. <https://doi.org/10.3390/molecules28020661>
- [3] NIST, *Definitions*. National Institute of Standards and Technology. <https://www.nist.gov/el/intelligent-systems-division-73500/definitions>, 2009.
- [4] H. Altug, S.-H. Oh, S. A. Maier, and J. Homola, "Advances and applications of nanophotonic biosensors," *Nature Nanotechnology*, vol. 17, no. 1, pp. 5-16, 2022. <https://doi.org/10.1038/s41565-021-01045-5>
- [5] S. Tabassum, S. Nayemuzzaman, M. Kala, A. Kumar Mishra, and S. K. Mishra, "Metasurfaces for sensing applications: Gas, bio and chemical," *Sensors*, vol. 22, no. 18, p. 6896, 2022. <https://doi.org/10.3390/s22186896>
- [6] V. Veselago, "The electrodynamic of substances with simultaneously negative values of and," *Soviet Physics Uspekhi*, vol. 92, no. 3, pp. 517-526, 1967. <https://doi.org/10.1070/pu1968v010n04abeh003699>
- [7] D. R. Smith, J. B. Pendry, and M. C. Wiltshire, "Metamaterials and negative refractive index," *Science*, vol. 305, no. 5685, pp. 788-792, 2004. <https://doi.org/10.1126/science.1096796>
- [8] C. Jansen, I. A. Al-Naib, N. Born, and M. Koch, "Terahertz metasurfaces with high Q-factors," *Applied Physics Letters*, vol. 98, no. 5, p. 051107, 2011. <https://doi.org/10.1063/1.3553193>
- [9] W. Cao, R. Singh, I. A. Al-Naib, M. He, A. J. Taylor, and W. Zhang, "Low-loss ultra-high-Q dark mode plasmonic Fano metamaterials," *Optics Letters*, vol. 37, no. 16, pp. 3366-3368, 2012. <https://doi.org/10.1364/ol.37.003366>
- [10] S. K. Patel, J. Parmar, V. Sorathiya, R. B. Zakaria, T. K. Nguyen, and V. Dhasarathan, "Graphene-based plasmonic absorber for biosensing applications using gold split ring resonator metasurfaces," *Journal of Lightwave Technology*, vol. 39, no. 17, pp. 5617-5624, 2021. <https://doi.org/10.1109/jlt.2021.3069758>
- [11] I. Abdalwahhab and I. Al-Naib, "Blood analysis method, US11,841,321," Retrieved: <https://patents.google.com/patent/US11841321B1/en>, 2023.
- [12] S. K. Patel, J. Surve, J. Parmar, K. Ahmed, F. M. Bui, and F. A. Al-Zahrani, "Recent advances in biosensors for detection of COVID-19 and other viruses," *IEEE Reviews in Biomedical Engineering*, vol. 16, pp. 22-37, 2022. <https://doi.org/10.1109/RBME.2022.3212038>
- [13] I. Al-Naib, "Sensing glucose concentration using symmetric metasurfaces under oblique incident terahertz waves," *Crystals*, vol. 11, no. 12, p. 1578, 2021. <https://doi.org/10.3390/cryst11121578>
- [14] V. Biswas and R. Vijaya, "Multi-modal flexible and inexpensive plasmonic metasurface for wide range of refractive index sensing," *Journal of Physics: Photonics*, vol. 6, no. 4, p. 045004, 2024. <https://doi.org/10.1088/2515-7647/ad6963>
- [15] A. Keshavarz and Z. Vafapour, "Water-based terahertz metamaterial for skin cancer detection application," *IEEE Sensors Journal*, vol. 19, no. 4, pp. 1519-1524, 2018. <https://doi.org/10.1109/JSEN.2018.2882363>
- [16] Z. Vafapour, A. Keshavarz, and H. Ghahraloud, "The potential of terahertz sensing for cancer diagnosis," *Heliyon*, vol. 6, no. 12, p. e05623, 2020. <https://doi.org/10.1016/j.heliyon.2020.e05623>
- [17] D. R. Shankaran, K. V. Gobi, and N. Miura, "Recent advancements in surface plasmon resonance immunosensors for detection of small molecules of biomedical, food and environmental interest," *Sensors and Actuators B: Chemical*, vol. 121, no. 1, pp. 158-177, 2007. <https://doi.org/10.1016/j.snb.2006.09.014>
- [18] M. Chakik, S. Bebe, and R. Prakash, "Hydrogenated graphene based organic thin film transistor sensor for detection of chloride ions as corrosion precursors," *Applied Sciences*, vol. 12, no. 2, p. 863, 2022. <https://doi.org/10.3390/app12020863>
- [19] M. R. Hasan and O. G. Hellesø, "Dielectric optical nanoantennas," *Nanotechnology*, vol. 32, no. 20, p. 202001, 2021.
- [20] P. Genevet, F. Capasso, F. Aieta, M. Khorasaninejad, and R. Devlin, "Recent advances in planar optics: From plasmonic to dielectric metasurfaces," *Optica*, vol. 4, no. 1, pp. 139-152, 2017.
- [21] A. Asim, M. Cada, A. Fine, Y. Ma, and F. Ibraheem, "Numerical investigation of a high-quality factor refractometric nano-sensor comprising all-dielectric metamaterial structures," *Coatings*, vol. 13, no. 6, p. 1027, 2023. <https://doi.org/10.3390/coatings13061027>
- [22] Y. Liang *et al.*, "Bound states in the continuum in anisotropic plasmonic metasurfaces," *Nano Letters*, vol. 20, no. 9, pp. 6351-6356, 2020. <https://doi.org/10.1021/acs.nanolett.0c01752>

- [23] S. Maier, *Plasmonics: Fundamentals and applications*. New York: Springer, 2007.
- [24] M. S. Bin-Alam *et al.*, "Ultra-high-Q resonances in plasmonic metasurfaces," *Nature Communications*, vol. 12, no. 1, p. 974, 2021. <https://doi.org/10.1038/s41467-021-21196-2>
- [25] B. Wang *et al.*, "High-Q plasmonic resonances: fundamentals and applications," *Advanced Optical Materials*, vol. 9, no. 7, p. 2001520, 2021. <https://doi.org/10.1002/adom.202001520>
- [26] L. Singh, P. Pareek, R. Kumar, V. Agarwal, N. K. Maurya, and A. Bage, "Investigation of SPR sensor for immunoglobulin detection by using Ag-Si 3 N 4-BP on the sensing layer," *Optical and Quantum Electronics*, vol. 56, no. 5, p. 771, 2024. <https://doi.org/10.1007/s11082-024-06665-4>
- [27] N. K. Maurya, P. Pareek, L. Singh, S. Kumari, and J. Ghosh, "Polarization-insensitive metasurface-biosensor for glycosuria sensing in Terahertz Regime," in *2024 IEEE Wireless Antenna and Microwave Symposium (WAMS)*, 2024: IEEE, pp. 1-5.
- [28] A. Asim and M. Cada, "Design of a plasmonic metasurface for refractive index sensing of aqueous glucose," *Progress In Electromagnetics Research Letters*, vol. 107, pp. 133-139, 2022. <https://doi.org/10.2528/piel22090401>
- [29] A. Asim, M. Cada, Y. Ma, and A. Fine, "Dual-resonance split ring resonator metasurface for terahertz biosensing," *IEEE Sensors Journal*, vol. 24, pp. 14189-14196, 2024.
- [30] H. Chen *et al.*, "High-sensitivity refractive index sensor based on strong localized surface plasmon resonance," *JOSA A*, vol. 41, no. 4, pp. 664-673, 2024.
- [31] B. Ni, G. Chu, Z. Xu, L. Hou, X. Liu, and J. Xiong, "High Q-factor, high contrast, and multi-band optical sensor based on plasmonic square bracket dimer metasurface," *Nanomaterials*, vol. 14, no. 5, p. 421, 2024. <https://doi.org/10.3390/nano14050421>
- [32] J. Wang, H. Shi, J. Xiao, and D. Bao, "High-Q-factor spoof localized surface plasmon sensor for MIM detection," in *2022 International Applied Computational Electromagnetics Society Symposium (ACES-China)*, 2022: IEEE, pp. 1-2.
- [33] M. Danaie, L. Hajshahvaladi, and E. Ghaderpanah, "A single-mode tunable plasmonic sensor based on an 8-shaped resonator for cancer cell detection," *Scientific Reports*, vol. 13, no. 1, p. 13976, 2023. <https://doi.org/10.1038/s41598-023-41193-3>
- [34] Y.-F. C. Chau *et al.*, "Simultaneous realization of high sensing sensitivity and tunability in plasmonic nanostructures arrays," *Scientific Reports*, vol. 7, no. 1, p. 16817, 2017.
- [35] N. Liu, M. Mesch, T. Weiss, M. Hentschel, and H. Giessen, "Infrared perfect absorber and its application as plasmonic sensor," *Nano Letters*, vol. 10, no. 7, pp. 2342-2348, 2010. <https://doi.org/10.1021/nl9041033>
- [36] M. R. Rakhshani and M. A. Mansouri-Birjandi, "High sensitivity plasmonic refractive index sensing and its application for human blood group identification," *Sensors and Actuators B: Chemical*, vol. 249, pp. 168-176, 2017. <https://doi.org/10.1016/j.snb.2017.04.064>
- [37] A. V. Kabashin *et al.*, "Plasmonic nanorod metamaterials for biosensing," *Nature Materials*, vol. 8, no. 11, pp. 867-871, 2009. <https://doi.org/10.1038/nmat2546>
- [38] L. Wu, H.-S. Chu, W. S. Koh, and E.-P. Li, "Highly sensitive graphene biosensors based on surface plasmon resonance," *Optics Express*, vol. 18, no. 14, pp. 14395-14400, 2010.
- [39] M. Xi, Q. Zhao, R. Duan, J. Yuan, Y. Quan, and H. Yang, "A reusable localized surface plasmon resonance biosensor for quantitative detection of serum squamous cell carcinoma antigen in cervical cancer patients based on silver nanoparticles array," *International Journal of Nanomedicine*, pp. 1097-1104, 2014. <https://doi.org/10.2147/ijn.s58499>
- [40] M. Mesch, C. Zhang, P. V. Braun, and H. Giessen, "Functionalized hydrogel on plasmonic nanoantennas for noninvasive glucose sensing," *Acs Photonics*, vol. 2, no. 4, pp. 475-480, 2015. <https://doi.org/10.1021/acsphotonics.5b00004>
- [41] Y. Li, *Plasmonic optics: Theory and applications*. SPIE. <https://doi.org/10.1117/3.2263757>, 2017.